PCCP

PAPER

View Article Online
View Journal | View Issue



Cite this: *Phys. Chem. Chem. Phys.*, 2016, **18**, 1578

# Mechanistic studies of pyridinium electrochemistry: alternative chemical pathways in the presence of $CO_2$†

A. G. Peroff, E. Weitz and R. P. Van Duyne*

Received 11th August 2015,
Accepted 20th November 2015

DOI: 10.1039/c5cp04757a

www.rsc.org/pccp

Protonated heterocyclic amines, such as pyridinium, have been utilized as catalysts in the electrocatalytic reduction of carbon dioxide. While these represent a new and exciting class of electrocatalysts, the details of the mechanism and faradaic processes occurring in solution are unclear. We report a series of cyclic voltammetry experiments involving Pt, Ag, Au, and Cu electrodes, under both aqueous and nonaqueous conditions, directed towards gaining an improved mechanistic understanding of pyridinium electrochemistry. Surface-enhanced Raman (SER) spectroelectrochemistry was also performed on Cu film-over-nanosphere electrodes in order to identify adsorbed species. It was found that the reduction potential of pyridinium (−0.58 V *vs.* SCE) and its electrochemical reversibility are unique features of platinum electrodes. In contrast, the reduction potentials on Ag, Au, and Cu electrodes are ~400 mV more negative than Pt in both the presence and the absence of $CO_2$. SER spectroelectrochemistry of pyridinium solutions shows no evidence for a pyridinium radical or a pyridinium ion. Increased cathodic current in the presence of $CO_2$ is only detected at scan rates less than 10 mV $s^{-1}$ in aqueous solutions. The addition of $CO_2$ resulted in a shift in the potential for the hydrogen evolution reaction. Pyridinium electrochemistry was observed under nonaqueous conditions; however no increase in cathodic current was observed when $CO_2$ was added to the solution. Based on this set of results it is concluded that the reduction potential of pyridinium is surface dependent, $CO_2$ acts as a pseudo-reserve of $H^+$, and pyridinium and $CO_2$ create an alternative mechanism for hydrogen evolution.

## I. Introduction

The need to develop environmentally benign sources of renewable energy represents one of the biggest challenges facing society.[1] A substantial part of our energy infrastructure runs on energy dense liquid fuels. While significant effort has been put into studies of the direct conversion of solar energy into electricity and into water splitting technologies, neither of these technologies directly yield energy dense hydrocarbon fuels. One solution to this problem is the electrochemical reduction of $CO_2$ to fuels.[2–5] While $CO_2$ reduction has the promise of producing energy dense hydrocarbon fuels, it is plagued by very low efficiencies, making it unusable at present for large scale production.[6] A better molecular level understanding of the mechanism for $CO_2$ reduction to fuels could reveal strategies that would allow for an increase in the efficiency of this process.

Recently, protonated heterocyclic amines such as pyridinium and imidazolium have been implemented as $CO_2$ reduction electrocatalysts.[7–9] Pyridinium has attracted much attention due to its reported conversion of $CO_2$ into methanol in both electrocatalytic and photoelectrocatalytic systems.[7,8] The first report of pyridinium electrocatalysis for $CO_2$ reduction was in 1994[10] using a hydrogenated Pd electrode. At that time, it was postulated that an irreversibly formed pyridinium radical acted as the electrocatalyst for $CO_2$ reduction.[10] In 2010, a more thorough study of pyridinium electrocatalysis on Pt electrodes was reported using electrochemical techniques, digital simulations, and density functional theory.[8] This study postulated that a pyridinium ion can undergo reversible $1e^-$ transfer to form a pyridinium radical, followed by six sequential steps in which a pyridinium radical donates an $H^+$ and a $1e^-$ ultimately reducing $CO_2$ to methanol.[8]

However, theoretical studies suggest that the redox potential for the formation of a pyridinium radical is too negative to be formed under the reported experimental conditions.[8,11–14] As a result of this discrepancy several different theoretical mechanisms have been postulated that could be thermodynamically feasible.[12,13,15,16] The most widely accepted mechanism at present was proposed by Batista and involves the formation of adsorbed hydrogen on Pt, which reduces $CO_2$.[13] Batista's

*Department of Chemistry, Northwestern University, 2145 Sheridan Road, Evanston, Illinois, 60208, USA. E-mail: vanduyne@northwestern.edu*

† Electronic supplementary information (ESI) available. See DOI: 10.1039/c5cp04757a

 

mechanism is supported by several experimental cyclic voltammetry studies which find evidence for the formation of adsorbed hydrogen on the electrode surface.[17,18] It should be noted that this mechanism only describes the conversion of $CO_2$ into formic acid, which is an intermediate in the formation of methanol.

Experimental insight into the mechanism of $CO_2$ reduction using pyridinium and other protonated heterocyclic amines has largely been based on cyclic voltammetry experiments. In one study the rate law for pyridinium electrocatalysis was determined from the increasing cathodic current when $CO_2$ was added to a pressurized electrochemical cell, with the conclusion that electrocatalysis is 1st order in pyridinium and 1st order in $CO_2$.[19] The electrocatalytic activity of other heterocyclic amines, imidazole and pyrazine was determined based on increased cathodic current in the cyclic voltammogram when $CO_2$ was added.[9,20] However, the faradaic efficiencies reported for methanol production using bulk electrolysis of pyridinium and $CO_2$ on metal electrodes ranged from $\sim$9% to $\sim$20%[8,20,21] and $\sim$3.6% for electrolysis of pyridazinium.[20] This suggests that the current mechanism for pyridinium catalysed $CO_2$ reduction on metal electrodes only accounts for $\sim$20% of the faradaic process interpreted from cyclic voltammograms, leaving $\sim$80% of the faradaic process unaccounted for. If protonated heterocyclic amines are to be used as catalysts for $CO_2$ reduction, a complete understanding of the faradaic process is desirable and should lead to strategies for improvements in the faradaic efficiency for conversion of $CO_2$ to methanol.

In this paper cyclic voltammetry experiments using Pt, Ag, Au and Cu electrodes in both aqueous and nonaqueous solutions are reported. Additionally, we have carried out surface-enhanced Raman (SER) spectroelectrochemistry of pyridinium on copper film-over-nanosphere (CuFON) electrodes aimed at the detection of any adsorbed species. We find that the reduction of pyridinium occurs on Ag, Au, and Cu as well as on Pt; however the peak cathodic current is shifted $\sim$400 mV more negative than Pt. Additionally, Pt is the only electrode that demonstrates reversible pyridinium cyclic voltammetry. Ag, Au and Cu electrodes show irreversible pyridinium cyclic voltammograms. SER spectroelectrochemistry on CuFONs shows only the Raman spectrum of pyridine: there was no evidence for adsorbed pyridinium or pyridinium radicals. Cathodic currents increased in the presence of $CO_2$ in aqueous solution; but no change in the cathodic current was observed under nonaqueous conditions. Additionally, the cathodic current in the presence of $CO_2$ only increased at slow scan rates (5 and 10 mV $s^{-1}$) under aqueous conditions. The addition of $CO_2$ to the aqueous pyridinium electrochemical system also shifts the onset of hydrogen evolution to less negative potentials on Pt, Ag, Au, and Cu electrodes. Based on these results, we propose a mechanism for alternative chemical processes taking place in addition to the reported electrocatalytic reduction of $CO_2$ in pyridinium solution. Pyridinium is reduced to adsorbed hydrogen on the electrode surface which oxidizes on Pt electrodes. $CO_2$ acts as an additional source of acid during electrolysis, increasing the concentration of pyridinium in solution. The potential for $H^+$ reduction shifts to less negative potentials in the presence of $CO_2$ which we attribute to water interacting with adsorbed hydrogen.

# II. Results

## A. Cyclic voltammetry of pyridinium on Pt, Ag, Au, and Cu electrodes in $H_2O$ without $CO_2$

30 mM pyridine was dissolved in 0.5 M KCl in water. The solution was acidified with 1 M $H_2SO_4$ until the pH was equal to 5.6 $\pm$ 0.02. Irreversible peak cathodic currents were observed in aqueous pyridinium solutions for Ag, Au, and Cu electrodes at $\sim -1.1$, $-0.9$, and $-1.0$ V *vs.* Ag/AgCl (Fig. 1). Reversible cyclic voltammograms of pyridinium were observed on Pt electrodes with a peak cathodic current at $-0.6$ V *vs.* Ag/AgCl, which is in agreement with previously reported pyridinium reduction electrochemistry (Fig. 1).[8] Additionally, bubbles were observed from all electrodes during the cathodic wave of the scan, which has previously been assigned as hydrogen gas.[8] Diffusion coefficients were experimentally determined from the peak cathodic current *vs.* the square root of the scan rate, in accordance with the Randles–Sevcik equation, and can be found in the ESI† (S1–S4).[22] The electrodes were ''benchmarked'' against hexaammineruthenium(III) chloride, which has been well established as a reversible homogeneous electroactive species, and has been used as a standard by other electrochemists.[23–28] As expected, for hexaammineruthenium(III) chloride, regardless of which electrode was used, the reversible current response was exactly the same for Pt, Ag and Au electrodes (S4–S7). Our cyclic voltammetry results for pyridinium show large differences in the shape and potential of the wave for each of the electrodes employed. This implies that pyridinium electrochemistry is substrate specific. However, we found a linear correlation between the peak cathodic current and the square root of the scan rate (S8–S11), as expected for an outer-sphere electron transfer process.[22] Thus, pyridinium electrochemistry is neither completely homogenous nor heterogeneous, but involves aspects of both.

## B. Cyclic voltammetry of pyridinium on Pt, Ag, Au, and Cu electrodes in $H_2O$ with and without $CO_2$

Cyclic voltammetric experiments on pyridinium in the presence of $CO_2$ were run using Pt, Ag, Au, and Cu electrodes. 30 mM

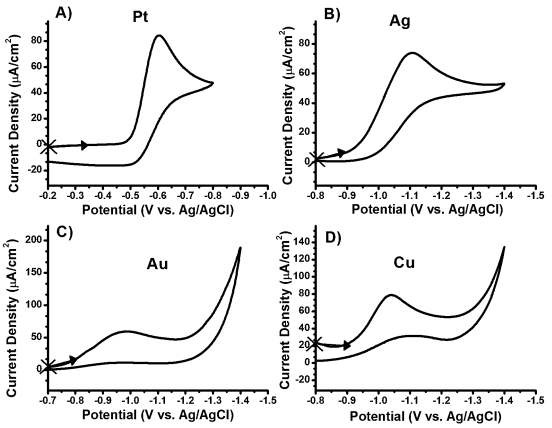


Fig. 1 Cyclic voltammetry of 30 mM pyridine in 0.5 M KCl dissolved in water at pH 5.6 on Pt (A), Ag (B), Au (C), and Cu (D) electrodes. All scan rates were 5 mV $s^{-1}$ and degassed in $N_2$.

pyridine was dissolved in 0.5 M KCl in water. $CO_2$ was bubbled through the solution until the solution reached 5.6 ± 0.02 pH units. $H_2SO_4$ was not added to solutions bubbled with $CO_2$. The current measured for pyridinium solutions with $CO_2$ was compared to pyridinium in the absence of $CO_2$ on all electrodes at 5 and 50 mV $s^{-1}$ (Fig. 2). At 5 mV $s^{-1}$ the peak cathodic current was ~25% larger in the presence of $CO_2$.

At 50 mV $s^{-1}$ there was little to no increase in the peak cathodic current. In general, scan rates greater than 10 mV $s^{-1}$ produced increased peak cathodic currents of ~5% or less in the presence of $CO_2$. S-shaped cyclic voltammograms were observed at slow scan rates and in the presence of $CO_2$: no S-shaped cyclic voltammograms were observed when $N_2$ was bubbled into the corresponding solutions. The addition of $CO_2$ also shifts the onset of the hydrogen evolution reaction (HER) (the rapid increase in current toward the endpoint of the forward sweep) to less negative potentials by 50 to 200 mV depending on the electrode. The pH for pyridinium solutions, with and without $CO_2$, is within ±0.02 pH units of each other, so pH cannot be responsible for changes in the onset potential for the hydrogen evolution reaction. This observed change in onset potential with the addition of $CO_2$ suggests that an alternative pathway for HER is operative.

While the shape of the cyclic voltammograms for all the electrodes studied is different, only Pt shows reversibility. Even when the reverse sweep was scanned to far less negative potentials than the starting potential, no anodic wave was observed on Ag, Au and Cu electrodes. On Pt, successively more negative potentials (−0.8, −0.9, −0.95, −1.0, and −1.05 V *vs.* Ag/AgCl) were swept in the absence of $CO_2$ to induce a rapid current increase associated with the $H^+$ reduction (Fig. 3).

The anodic wave at −0.5 V and −0.85 V increased with each successive scan and was only observed on Pt electrodes, suggesting that the oxidation processes are surface specific and related to $H^+$ reduction.

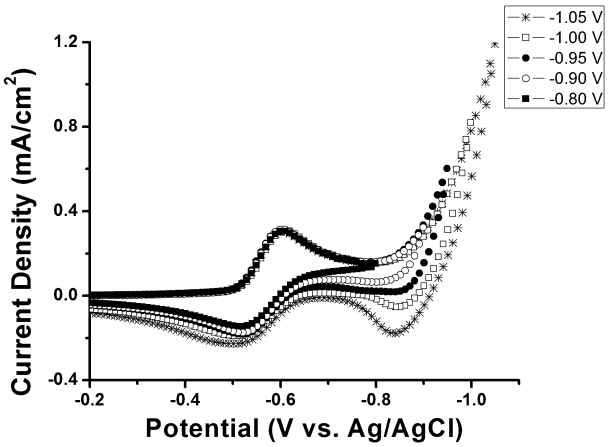


Fig. 3 Cyclic voltammetry of 30 mM pyridinium in 0.5 M KCl dissolved in water at pH 5.6 on a Pt electrode at 100 mV $s^{-1}$ degassed in $N_2$. Cyclic voltammograms were swept from −0.2 to −0.8 (black squares), −0.9 (white circles), −0.95 (black circles), −1.0 (white squares), and −1.05 V (stars).

### C. Cyclic voltammetry of pyridinium on Pt, Ag, Au and Cu electrodes in acetonitrile with and without $CO_2$

Pyridinium electrochemistry in acetonitrile in the absence of $CO_2$ showed similar results to the aqueous system. A reversible cyclic voltammogram with a peak cathodic current at −0.6 V *vs.* Ag wire QRE was observed on Pt and an irreversible cyclic voltammogram with a peak cathodic current at −1.3, −1.2, and −1.35 V *vs.* Ag wire QRE was also used for Ag, Au and Cu electrodes, respectively (S12–S15). Additionally, hydrogen bubble formation was observed during cyclic voltammetry scans for all electrodes, which is consistent with previous reports.[29] However, when $CO_2$ was added, no increase in cathodic current at slow scan rates was observed as was seen for the aqueous system (Fig. 4). This is surprising in light of the report that the electrocatalytic reduction of $CO_2$ is 1st order in pyridinium concentration and 1st order in $CO_2$ concentration.[19] A testable consequence of the 1st order kinetics in $CO_2$ is to perform electrochemistry in acetonitrile, where the concentration of $CO_2$ is ~8 times larger (~280 mM) than in water.[30] Thus an increase in the cathodic current by a factor of 8 would be anticipated, however no change or a small decrease in current was observed. This suggests that the increase in cathodic current with the addition of $CO_2$ is solvent dependent.

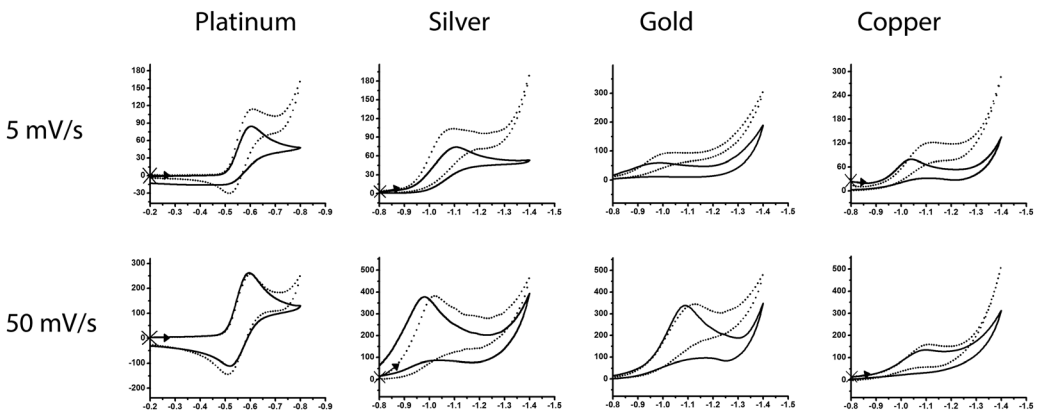


Fig. 2 Comparison of cyclic voltammograms with $CO_2$ (dotted line). 30 mM pyridine in 0.5 M KCl dissolved in water at pH 5.6. Pt, Ag, Au, and Cu electrodes were used. Cyclic voltammograms on the top and bottom row were performed at 5 mV $s^{-1}$ and 50 mV $s^{-1}$, respectively.

 

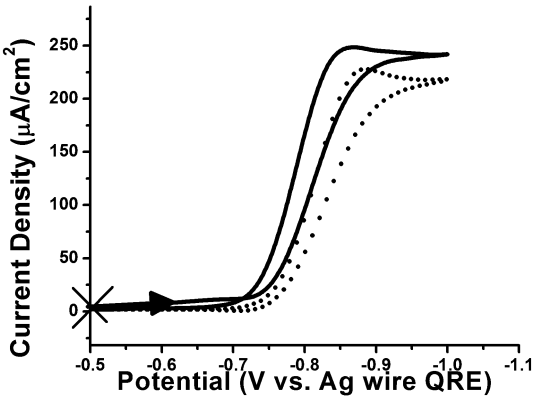


Fig. 4 Cyclic voltammetry of 30 mM pyridine and 30 mM perchloric acid, in 0.5 M $NaClO_4$ dissolved in acetonitrile on a Pt electrode at 5 mV $s^{-1}$, saturated with $CO_2$ (dotted line) and with $N_2$ (solid line).

### D. SER spectroelectrochemistry of pyridinium on Cu

In addition to mechanistic pathways, the identification of possible species on the electrode surface was of interest. Multiple species such as a pyridinium radical and dihydropyridine have been proposed as the active catalyst for $CO_2$ reduction; however there has been no experimental detection of either species.[8,15,16] SER spectroelectrochemistry was used to probe the electrode surface. Pyridine and pyridinium Raman spectroelectrochemistry was performed on CuFON electrodes (Fig. 5). The pyridine solution consisted of 50 mM pyridine in 0.1 M KCl which are the same conditions used in previous SER spectroelectrochemistry experiments.[31,32] The pyridinium solution consisted of 30 mM pyridine in 0.5 M KCl at pH 5.6 (the same as in the aqueous electrochemistry experiments). Both spectra in Fig. 5 were taken at −1 V *vs.* Ag/AgCl, where the cathodic current onset occurs on copper electrodes.

There is a 2.5 times increase in the signal for the pyridine solution relative to the pyridinium solution, which is due to the increase in pyridine concentration between the two solutions. The 1012 $cm^{-1}$ ring breathing mode would be different for pyridine, pyridinium, dihydrogen pyridine, and the pyridinium radical.[32] However, there was no such change in the frequency of the ring breathing mode between the pyridine and pyridinium solution spectra. This suggests that only pyridine and not pyridinium, dihydropyridine, nor a pyridinium radical is adsorbed on the Cu electrode surface. While this study was performed on CuFON electrodes, the adsorption of pyridine on the electrode surface extends to Ag, Au, and Pt electrodes. There have been numerous studies of SERS spectroelectrochemistry of pyridine on Ag and Au electrodes.[31–35] Even surface Raman of pyridine on a Pt electrode was performed, where pyridine was adsorbed on the Pt surface.[36] Even though the solution conditions are different between SERS spectroelectrochemical experiments of pyridine in the literature, the adsorption of pyridine on the electrode surface is the same. The formation of an adsorbed layer of pyridine is also supported by electrochemistry experiments by Shaw, where a reversible redox wave was observed prior to the pyridinium redox wave, indicative of a layer of adsorbed pyridine on an Au electrode.[37]

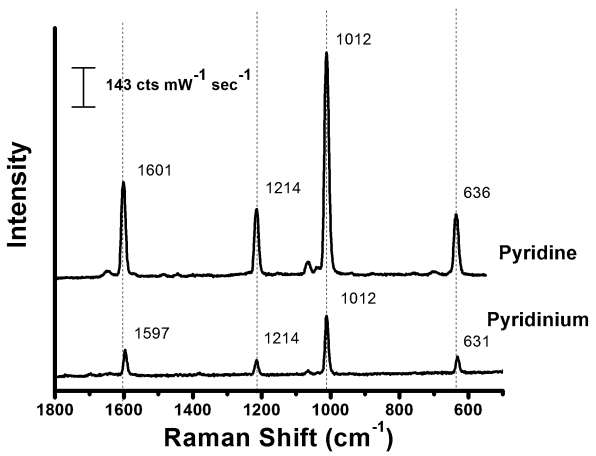


Fig. 5 Raman spectroelectrochemistry of 30 mM pyridine in 0.5 M KCl dissolved in water at pH 5.6 (bottom spectra) and 50 mM pyridine in 0.1 M KCl dissolved in water (top spectra). Cu film over the nanosphere (CuFON) electrode was employed. Spectra were collected using a 633 nm HeNe laser at 7 mW with 1 s acquisition time. Both pyridine and pyridinium solutions were held at −1 V *vs.* Ag/AgCl.

## III. Discussion

The observed potential shift for Ag, Au, and Cu electrodes from Pt can be explained by the HER which forms adsorbed hydrogen as an intermediate (eqn (1) and (2)), where eqn (2) is the Volmer–Tafel reaction.

$$H^+ + e^- \rightarrow H_{(ads)} \quad (1)$$

$$H_{(ads)} + H_{(ads)} \rightarrow H_{2(g)} \quad (2)$$

The mechanism for the HER in acidic solutions has been extensively studied on various electrodes.[38–41] Ag, Au, and Cu have been reported to have similar HER potentials (depending on the crystal face), as well as potentials far more negative than observed on Pt,[42] both of which follow the same order as the reduction potential of pyridinium on Pt, Ag, Au and Cu electrodes. Belanger has found a similar trend with Pt, Ir, Au and glass carbon electrodes for pyridinium electrochemistry.[18] However, Belanger assigned the cyclic voltammetry response for Pt and Ir to the reduction of pyridinium to adsorbed hydrogen, while the cyclic voltammetry response for Au and glassy carbon electrodes was assigned to the formation of a pyridinium radical.[18] Shaw also has recently reported the reduction of pyridinium on Au to a pyridinium radical as well.[37] Assigning pyridinium reduction to a homogeneous pyridinium radical presents two problems. (1) The reduction potential for a diffusion controlled homogeneous electroactive species should be independent of the electrode material, such as the case of hexaammineruthenium(III) chloride. (2) Several independent theoretical studies have calculated the reduction potential of a pyridinium radical to be ~−1.4 V *vs.* SCE, which is ~400 mV more negative than the observed reduction potential.[37] The assignment of pyridinium reduction to adsorbed hydrogen is consistent across all electrode surfaces. This is in agreement with Belanger's description that the difference in

reduction potential correlates with the metal–hydrogen bond energy.[18] The irreversibility of Ag, Au, and Cu can be attributed to the rapid dissociation of weakly bound adsorbed hydrogen. We performed digital simulations for pyridinium electrochemistry on Pt, Ag, Au, and Cu electrodes using a reversible $1e^-$ transfer followed by an irreversible chemical step. Our simulations show the rate for the chemical step to be $>10\ s^{-1}$ for Ag, Au and Cu, while only $0.11\ s^{-1}$ for Pt (S8–S11). The $\sim -400$ mV more negative potential increases the mobility of adsorbed hydrogen, resulting in a larger rate for the formation of hydrogen gas. This irreversible chemical process does not allow for oxidation to occur on Ag, Au, and Cu electrodes. In addition to our results, Bocarsly has performed cyclic voltammetry on a variety of weak acids (such as pyridinium) on Pt, and found a linear correlation between the reduction potential and the $pK_a$, suggesting that $H^+$ is being reduced at the surface.[17] Based on this evidence, the reduction potential of pyridinium directly correlates with the formation of adsorbed hydrogen on the electrode surface, consistent with Batista's mechanism.

It was originally postulated that the reversible $1e^-$ transfer from a pyridinium radical gave rise to the anodic wave observed on Pt.[8] Experimentally, platinum electrodes were the only electrodes that showed reversibility for pyridinium in both aqueous and acetonitrile solutions. Instead of a pyridinium radical, the anodic wave corresponds to the oxidation of adsorbed hydrogen atoms by Pt. Our study suggests that two oxidation processes are occurring. As shown in Fig. 3, cyclic voltammograms of pyridinium on Pt electrodes in the absence of $CO_2$ from $-0.2$ V to $-0.8$, $-0.9$, $-0.95$, $-1.0$, and $-1.05$ V *vs.* Ag/AgCl show two anodic waves at $-0.5$ and $-0.85$ V. During the forward sweep from $-0.2$ to $-0.8$ V *vs.* Ag/AgCl, all the cyclic voltammograms have excellent overlap with each other. As more hydrogen is evolved at more negative potentials, the anodic waves at $-0.5$ and $-0.85$ V *vs.* Ag/AgCl increase. The rapid increase of cathodic current in the forward sweep is hydrogen evolution from water dissociation. More acidic species such as $H_3O^+$ and pyridinium, have lower reduction potentials than the rapid increase at $\sim -0.9$ V *vs.* Ag/AgCl that is observed on Pt electrodes. The result of $H^+$ reduction associated with water dissociation leaves hydroxyl groups on the surface of Pt. Hydroxyl groups are either oxidized during the reverse sweep at $-0.85$ V *vs.* Ag/AgCl or they remain on the electrode surface. Oxidation of a fraction of the hydroxyl groups would be expected for a reaction with a finite rate constant and the modest sweep rate ($100\ mV\ s^{-1}$) employed. The hydroxyl groups that are not oxidized change the electrochemical double layer, resulting in an increase in the background current during the reverse sweep. This is observed in the cyclic voltammogram between $\sim -0.75$ and $\sim -0.6$ V *vs.* Ag/AgCl, where the amplitude of the background current changes as a function of the negative endpoint of the sweep. This increase in background current explains the observed increase in the current of the anodic wave at $-0.5$ V *vs.* Ag/AgCl. The anodic wave at $-0.5$ V is assigned to the oxidation of adsorbed hydrogen to $H^+$, which subsequently reacts with pyridine to form pyridinium (eqn (3) and (4)). This leads to an increase in the pyridinium concentration at the electrode surface compared to the bulk, which results in the diffusion of pyridinium away from the electrode surface. This oxidation process at $-0.5$ V was not observed on Ag, Au, and Cu electrodes and is assigned as a unique feature of Pt as a result of oxidation of adsorbed hydrogen.[43–45]

$$H_{(ads)} + Pt \rightarrow H^+ + Pt + e^- \quad (3)$$

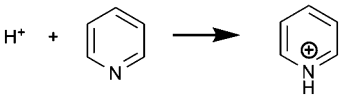

(4)

An important observation based on the data from Fig. 2 is the dependence of the cathodic current on the scan rate in the presence of $CO_2$. For all electrodes the increased cathodic current and the S-shape of the cyclic voltammograms were only observed at slow scan rates (5 and $10\ mV\ s^{-1}$) in the presence of $CO_2$. At faster scan rates there is little or no increase in cathodic current. In fact, most of the cyclic voltammograms reported in the literature for the electrocatalytic reduction of $CO_2$ using pyridinium were taken at either $1\ mV\ s^{-1}$ [8] or $5\ mV\ s^{-1}$.[18,19] The increase in cathodic current in the presence of $CO_2$ has been commonly used as a means of measuring catalytic activity. Further to this point, Saveant suggested that the increase in cathodic current is not due to $CO_2$ reduction but rather to the superposition of $H^+$ from carbonic acid and pyridinium being reduced.[46] The results from the nonaqueous pyridinium experiments suggest that the increase in cathodic current observed in the aqueous pyridinium experiments with $CO_2$ is attributed to additional pyridinium formed from a shift in carbonic acid equilibrium. No carbonic acid is formed in acetonitrile and no increase in cathodic current was observed. If the increase in cathodic current were due to electrocatalysis, then a large increase in the cathodic current would be expected, as the concentration of $CO_2$ is $\sim 8$ times larger in acetonitrile than in water. A recent study by Sariciftci on pyridinium and pyridazinium with and without $CO_2$ supports the claim that the increase in cathodic current is due to additional pyridinium formed from a shift in carbonic acid equilibrium.[20] Pyridazinium cathodic current was 5 times larger in the presence of $CO_2$ than without $CO_2$, while pyridinium showed only an $\sim 5\%$ increase in cathodic current in the presence of $CO_2$. However, bulk electrolysis experiments showed more methanol production using pyridinium than pyridazinium.[20] This calls into question the correlation between electrocatalytic activity and the increase in cathodic current when $CO_2$ is added to protonated heterocyclic amine solutions. Additionally, the pH of the pyridinium solution was 5.3 while that of pyridazinium was 4.7. While this is only a 0.6 pH unit difference it corresponds to a 5 fold difference in $[H^+]$. The resulting shift in carbonic acid equilibrium would increase the carbonic acid concentration by 5 times, which corresponds to the difference in cathodic current for pyridazinium with and without $CO_2$. The assignment of heterocyclic amines as electrocatalysts[20] and kinetic studies of pyridinium electrocatalysis[19] were based on assigning the increased cathodic current to $CO_2$ reduction, rather than the formation of carbonic acid. The rate law for pyridinium electrocatalysis was determined by performing

 

electrochemistry in a pressurized electrochemical cell.[19] Varying pressures of $CO_2$ were added to the electrochemical cell in the presence of pyridine and the change in cathodic current was measured as a function of increasing $CO_2$ pressure. A linear dependence of cathodic current with added $CO_2$ was reported, and it was concluded that pyridinium electrocatalysis was 1st order in $CO_2$. However, the increased cathodic current in the presence of $CO_2$ is due to additional pyridinium formed from a shift in carbonic acid equilibrium, not from electrocatalysis. As a result, the rate law for pyridinium electrocatalysis cannot be determined from this study.

While the increase in cathodic current is due to carbonic acid, it was found that it is not due to the reduction of carbonic acid to adsorbed hydrogen or hydrogen gas. Assigning the increase in cathodic current specifically to carbonic acid reduction presents two problems. (1) Why would the reduction potential of carbonic acid be the same as pyridinium? Bocarsly demonstrated that the redox potential for a series of weak acids shifts as a function of the p$K_a$;[17] the p$K_a$ of carbonic acid is 6.35 while the p$K_a$ of pyridinium is 5.17. (2) $CO_2$ bubbled into a pH 5.3 buffer solution in the absence of pyridine does not show any cathodic current (S16).

A more accurate description for the increase of cathodic current in the presence of $CO_2$ requires a careful examination of the dynamic equilibrium achieved in solution. Acidification of pyridine to pyridinium in the absence of $CO_2$ comes from the addition of sulfuric acid, which completely dissociates in solution. In the presence of $CO_2$, acidification of pyridine to pyridinium comes from the formation of carbonic acid (eqn (5)–(7)). For an accurate comparison of the two solutions, the pH of both solutions must be equal. This involves sufficient bubbling of $CO_2$ into a pyridine solution, until equilibrium is established between $H_3O^+$, pyridinium and carbonic acid. The pyridine solution in the absence of $CO_2$ is acidified with $H_2SO_4$ until the pH is equal to that of the $CO_2$ saturated solution. The reduction of pyridinium to adsorbed hydrogen and pyridine causes a shift in equilibrium causing $H_3O^+$ to protonate pyridine. In the solution without $CO_2$, the only source of $H_3O^+$ comes from $H_2SO_4$. However, in the $CO_2$ saturated solution, $H_3O^+$ comes from carbonic acid. When carbonic acid is consumed to form $H_3O^+$, it shifts the equilibrium toward carbonic acid. This leads to more carbonic acid capable of making $H_3O^+$ to protonate pyridine. Based on the pyridine to pyridinium equilibrium (eqn (7)), a 0.01 pH unit change leads to a 2–3% change in the concentration of pyridinium, hence only a small amount of carbonic acid needs to deprotonate to demonstrate the observed 5–25% change in cathodic current. In a $CO_2$ saturated solution, carbonic acid effectively changes the pH by 0.2–0.8 units (depending on the scan rate), thus increasing the concentration of pyridinium during the cyclic voltammogram scan in the presence of $CO_2$. The formation of carbonic acid from $CO_2$ to water is a kinetically slow process, which explains why the increased cathodic current is only observed at slow scan rates (1–10 mV $s^{-1}$).[46] Incorporating the dynamic equilibrium of carbonic acid in solution is very important if protonated heterocyclic amines are to be investigated as potential $CO_2$ reduction electrocatalysts.

$$CO_2 + H_2O \rightleftharpoons H_2CO_3 \quad (5)$$

$$H_2CO_3 + H_2O \rightleftharpoons H_3O^+ + HCO_3^- \quad (6)$$

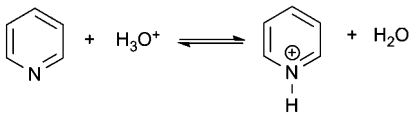


(7)

Data shown in Fig. 2 reveal another interesting phenomenon regarding the rapid increase in current observed at the endpoint of the forward sweep of the cyclic voltammogram. With the addition of $CO_2$ we observe a shift in the onset for $H^+$ reduction to less negative potentials. The magnitude of the shift varies from 50 to 200 mV depending on the electrode surface. In the case of Pt (5 and 50 mV $s^{-1}$) and Ag (5 mV $s^{-1}$) the onset of $H^+$ reduction was only observed during cyclic voltammetry scans with added $CO_2$. While the pH might change as a result of the carbonic acid equilibrium described above, the pH change is relatively minor compared to the magnitude of the potential shifts we observed. Based on the Nernst equation a pH change of 1 corresponds to a potential shift of 59 mV.[47] Potential shifts from 50 to 200 mV have been observed, suggesting that the pH would be changing from ~1–4 units. If the pH were changing between 1 and 4 units it would be expected that the cathodic current for pyridinium reduction increases several orders of magnitude, which is not the case. As mentioned previously, carbonic acid most likely only changes the pH by 0.2 to 0.8 units. The small change in pH from carbonic acid cannot be responsible for the large shift in potential for the current at the endpoint of the cyclic voltammogram. It is possible that carbonic acid itself is being reduced to adsorbed hydrogen and hydrogen gas. It was shown that the redox potential of weak acids on platinum is a function of p$K_a$.[17] The p$K_a$ of carbonic acid and pyridinium is 6.35 and 5.17, respectively, suggesting that the redox potential carbonic acid is roughly 100 mV more negative than pyridinium. It may be the case that carbonic acid reduction overlaps hydrogen evolution current during the cyclic voltammetry sweeps. The shift in potential suggests that the addition of $CO_2$ must be creating a thermodynamically more favorable pathway for $H^+$ reduction to $H_2$. Alternatively, the observed shift in potential could be due to $CO_2$ reduction. Assuming that $CO_2$ reduction is occurring at this potential, this would affect the potential that should be selected for bulk electrolysis studies.

While the exact assignment for the rapid increase in current is unknown, a hypothesis that would account for both $CO_2$ and $H^+$ reduction is based on Batista's mechanism. According to Batista's mechanism (Fig. 6), in the absence of $CO_2$ two pyridinium molecules are required to form hydrogen gas. In the presence of $CO_2$ only one adsorbed hydrogen is required to initiate $CO_2$ reduction.

This leaves a surface hydrogen available to react to form hydrogen gas. We hypothesize that instead of two water molecules reacting to form hydrogen and hydroxyl groups (eqn (8)), one adsorbed hydrogen atom reacts with water to form $H_2$ and a hydroxyl group on the electrode surface (eqn (9)).[44] The formation of hydrogen gas from one adsorbed hydrogen and

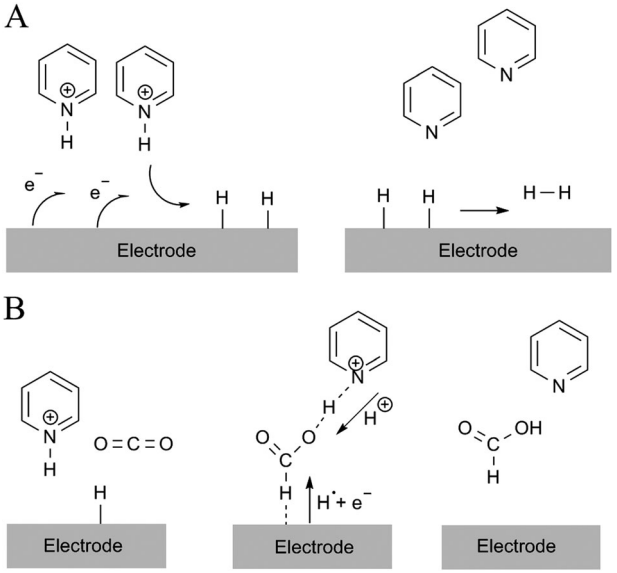


Fig. 6 Our depiction of the mechanism proposed by Batista where in the absence of $CO_2$, two pyridinium molecules reduce to form hydrogen (A). In the presence of $CO_2$ adsorbed hydrogen atoms interact with $CO_2$ to form a bent $HCO_2$ moiety which further reacts to gain a $H^+$ from pyridinium and $1e^-$ from the electrode to form formic acid, regenerating pyridine (B).

water (eqn (9)) is the Heyrovsky reaction, where water acts as the acid. Eqn (8) is the hydrolysis of water; whereas eqn (2) (Volmer–Tafel reaction) is an intermediate step in the process. DFT studies by Nørskov suggest that the transition state energy for the Tafel reaction is 0.55 eV; whereas, the Volmer–Heyrovsky reaction only has a transition state energy of $\sim$0.3 eV.[48] The lower energy barrier for the Volmer–Heyrovsky reaction might explain the shift in the potential of pyridinium solutions with added $CO_2$. The reaction of added $CO_2$ with adsorbed hydrogen *via* Batista's mechanism, limits the amount of adsorbed hydrogen that can produce hydrogen gas *via* the Volmer–Tafel reaction. The limited adsorbed hydrogen allows the Volmer–Heyrovsky reaction to be the dominant reaction mechanism for hydrogen evolution, leading to a shift in the HER potential. That being said, carbonic acid reduction to adsorbed hydrogen and subsequently hydrogen gas is another possibility that cannot be ruled out.

Based on the results of this study a more complete mechanism for pyridinium electrochemistry that accounts for alternative pathways to the formation of hydrogen gas is proposed. Our mechanism involves an electrode characterized by an adsorbed layer of pyridine, which is supported by the SER spectroelectrochemistry data. All of the mechanistic implications of an adsorbed pyridine layer are currently unclear, however it can be implied that the adsorbed layer of pyridine does not block further electrochemical processes, as they are observed in the experimental cyclic voltammograms. It may be possible that the adsorbed pyridine layer is slowing down kinetic processes such as eqn (2) where adsorbed hydrogen should rapidly combine to form hydrogen gas. This would allow sufficient time for some of the adsorbed hydrogen to oxidize on Pt electrodes, as observed by the anodic current.

$$2H_2O + 2e^- \rightarrow H_{2(g)} + 2OH^-_{(ads)} \quad (8)$$

$$H_2O + H_{(ads)} + e^- \rightarrow H_{2(g)} + OH^-_{(ads)} \quad (9)$$

The first step of our proposed mechanism involves the diffusion controlled reduction of pyridinium to form surface hydrogen, where the reduction potential is a function of the electrode surface (Fig. 7A). As a result, pyridinium rapidly loses $H^+$, forming pyridine. In the absence of $CO_2$, surface hydrogen combines to form hydrogen gas (Fig. 7B). The formation of hydrogen gas is more rapid on Ag, Au, and Cu electrodes,

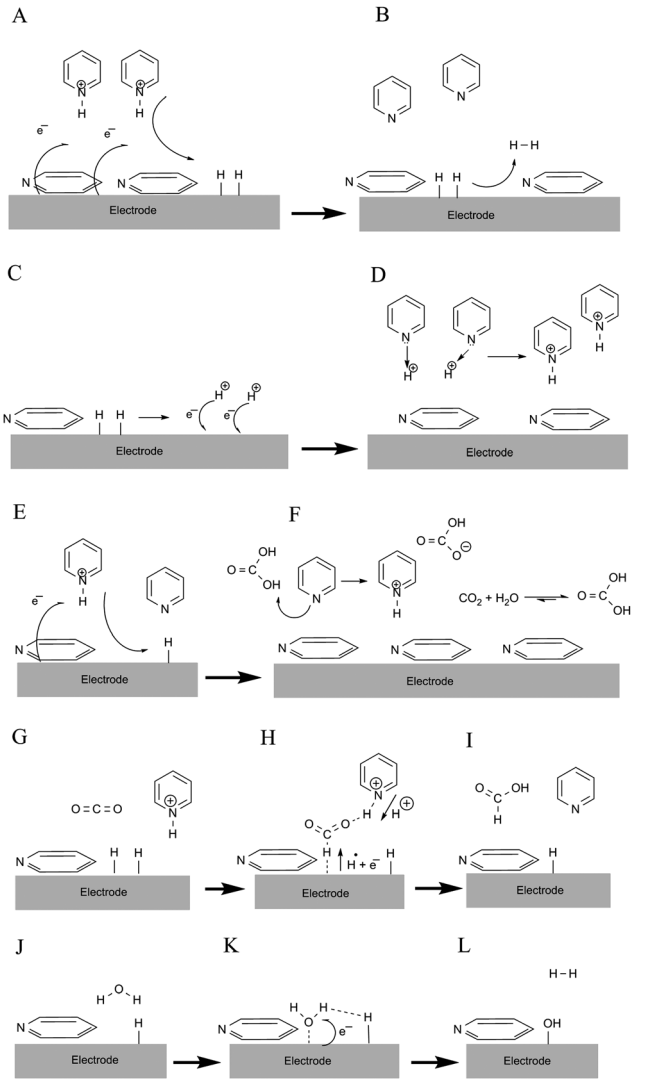


Fig. 7 Proposed mechanism describing pyridinium electrochemistry. (A to B) Diffusion of pyridinium toward the electrode surface, forming adsorbed hydrogen to hydrogen gas. (C to D) Adsorbed hydrogen is oxidized to $H^+$ which reacts with pyridine forming pyridinium. (E to F) In the presence of $CO_2$ carbonic acid protonates pyridine to pyridinium, and $CO_2$ + water regenerates carbonic acid. (G to I) Depiction of Batista's mechanism, which shows the additional adsorbed hydrogen after $CO_2$ reduction. (J to L) The remaining adsorbed hydrogen after step I reacts with $H_2O$ and $1e^-$ to form hydrogen gas and hydroxyl groups on the surface. During all steps of the mechanism there is adsorbed pyridine on the electrode surface.

 

leaving no available hydrogen atoms to oxidize during the reverse sweep. The anodic wave is only observed on platinum electrodes where surface hydrogen is oxidized to form $H^+$ which reacts with pyridine to form pyridinium (Fig. 7C and D). In the presence of $CO_2$, carbonic acid acidifies pyridine during the negative sweep which shifts the $CO_2$ equilibrium concentration to form more carbonic acid (Fig. 7E and F). To explain the increase in hydrogen evolution in the presence of $CO_2$, it is proposed that possibly $CO_2$ is reduced through Batista's mechanism (Fig. 7G–I), and/or unreacted surface hydrogen reacts with water to form hydrogen gas (Volmer–Heyrovsky) and hydroxyl groups at a less negative potential than would be required for $H^+$ reduction (Fig. 7J–L). The ~20% faradaic efficiency observed on metal electrodes for $CO_2$ reduction might be in-part due to the electrons used in this alternative pathway for hydrogen evolution.

## IV. Experimental methods

A three electrode potentiostat (CH660D CH instruments) was employed using a custom electrochemical cell.[49] Ag/AgCl was used as the reference electrode, and a Pt wire cleaned in fresh piranha solution (3 : 1 v/v concentrated $H_2SO_4$ to 30% $H_2O_2$) was employed as the counter electrode. Working electrodes consisted of flat disc Pt, Ag, Au and Cu electrodes with a 2 mm diameter (CH instruments), which were sequentially polished in 1, 0.3, and 0.05 μm alumina powder slurries, using a polishing wheel, until the electrodes acquired a mirror like shine. Working electrodes were sonicated in MilliQ water (Millipore) and dried between polishing and prior to electrochemistry experiments. Two types of aqueous pyridine solutions were prepared, one with $CO_2$ and one without $CO_2$. Both solutions consisted of 30 mM pyridine (Aldrich) dissolved in a 0.5 M KCl (Aldrich) solution with MilliQ water as the solvent. When $CO_2$ is added, carbonic acid forms in solution, which protonates pyridine to form pyridinium and results in a pH decrease from 8.0 to ~5.6. In the absence of $CO_2$, 1 M $H_2SO_4$ was added dropwise to aqueous pyridine solutions until the pH equalled ~5.6 (±0.02 pH units). The $K_a$ for pyridinium is $6.76 \times 10^{-6}$.[8] Consequently, the calculated pyridinium concentration in the presence and the absence of $CO_2$ is ~10 mM. Aqueous electrochemistry experiments were benchmarked against 5 mM hexaammineruthenium(III) chloride (Strem Chemicals) solutions. The composition of the solution for nonaqueous studies consisted of 30 mM pyridine, 30 mM perchloric acid, and 0.5 M sodium perchlorate in acetonitrile (Honeywell BJ). An Ag wire quasi reference electrode (QRE) was employed for all nonaqueous studies. All gases bubbled into solutions prior to electrochemistry experiments were ultra-high purity $N_2$, $CO_2$, or $H_2$. Digital simulations were performed on aqueous pyridinium solutions using DigiElch version 6.F. The experimental details for the SER spectroelectrochemistry experiments can be found in the ESI† (S17).

## V. Conclusions

We performed a series of experiments aimed at understanding chemical pathways in pyridinium electrochemistry which are alternatives to $CO_2$ reduction. The reduction potential for pyridinium electrochemistry in the absence of $CO_2$ corresponds to the reduction of pyridinium to adsorbed hydrogen and is a function of the electrode material. Irreversible cathodic current was observed on Ag, Au, and Cu electrodes at ~400 mV more negative than Pt in aqueous and acetonitrile pyridinium solutions. The oxidation of adsorbed hydrogen is only observed on Pt electrode and manifests itself as the anodic wave in the cyclic voltammetry of pyridinium. The increase in cathodic current with the addition of $CO_2$ was only observed at slow scan rates on all electrodes, and was not observed in acetonitrile solutions. This increase in cathodic current is most likely due to carbonic acid donating $H^+$ to pyridinium during the cyclic voltammogram scan.

The shift in the onset potential for the hydrogen evolution reaction was observed on all electrodes in the presence of $CO_2$. This shift in potential suggests an alternative pathway for $H^+$ reduction. If $CO_2$ reduction were occurring near the HER potential, it would affect the potential that should be applied to optimize $CO_2$ reduction during bulk electrolysis.

Based on these data a mechanism has been developed, shown in Fig. 7, for pyridinium electrochemistry. The mechanism indicates that dynamic chemical equilibria need to be taken into consideration when analysing electrochemical data of heterocyclic amines as potential $CO_2$ reduction catalysts.

## Acknowledgements

This work was supported by the Chemical Sciences, Geosciences, and Biosciences Division, Office of Basic Energy Sciences, Office of Science, U.S. Department of Energy (Award No. DE-FG02-03-ER154557) and in part by NSF CHE 08(CASTL)/Grant/Award # CHE-1414466 and AFOSR MURI Grant FA9550-14-1-003.

## References

1 N. Lewis and D. Nocera, *Proc. Natl. Acad. Sci. U. S. A.*, 2006, **103**, 15729.
2 G. Centi and S. Perathoner, *Top. Catal.*, 2009, **52**, 948.
3 D. T. Whipple and P. J. A. Kenis, *J. Phys. Chem. Lett.*, 2010, **1**, 3451.
4 G. Centi, E. A. Quadrelli and S. Perathoner, *Energy Environ. Sci.*, 2013, **6**, 1711.
5 G. A. Olah, G. K. S. Prakash and A. Goeppert, *J. Am. Chem. Soc.*, 2011, **133**, 12881.
6 S. C. Roy, O. K. Varghese, M. Paulose and C. A. Grimes, *ACS Nano*, 2010, **4**, 1259.
7 E. E. Barton, D. M. Rampulla and A. B. Bocarsly, *J. Am. Chem. Soc.*, 2008, **130**, 6342.
8 E. Barton Cole, P. S. Lakkaraju, D. M. Rampulla, A. J. Morris, E. Abelev and A. B. Bocarsly, *J. Am. Chem. Soc.*, 2010, **132**, 11539.
9 A. B. Bocarsly, Q. D. Gibson, A. J. Morris, R. P. L'Esperance, Z. M. Detweiler, P. S. Lakkaraju, E. L. Zeitler and T. W. Shaw, *ACS Catal.*, 2012, **2**, 1684.

10 G. Seshadri, C. Lin and A. B. Bocarsly, *J. Electroanal. Chem.*, 1994, **372**, 145.
11 J. A. Keith and E. A. Carter, *J. Am. Chem. Soc.*, 2012, **134**, 7580.
12 C.-H. Lim, A. M. Holder and C. B. Musgrave, *J. Am. Chem. Soc.*, 2012, **135**, 142.
13 M. Z. Ertem, S. J. Konezny, C. M. Araujo and V. S. Batista, *J. Phys. Chem. Lett.*, 2013, **4**, 745.
14 J. A. Tossell, *Comput. Theor. Chem.*, 2011, **977**, 123.
15 J. A. Keith and E. A. Carter, *Chem. Sci.*, 2013, **4**, 1490.
16 J. A. Keith and E. A. Carter, *J. Phys. Chem. Lett.*, 2013, 4058.
17 Y. Yan, E. L. Zeitler, J. Gu, Y. Hu and A. B. Bocarsly, *J. Am. Chem. Soc.*, 2013, **135**, 14020.
18 E. Lebègue, J. Agullo, M. Morin and D. Bélanger, *ChemElectroChem*, 2014, **1**, 1013.
19 A. J. Morris, R. T. McGibbon and A. B. Bocarsly, *ChemSusChem*, 2011, **4**, 191.
20 E. Portenkirchner, C. Enengl, S. Enengl, G. Hinterberger, S. Schlager, D. Apaydin, H. Neugebauer, G. Knör and N. S. Sariciftci, *ChemElectroChem*, 2014, **1**, 1543.
21 E. Barton Cole, M. Baruch, R. L'Esperance, M. Kelly, P. Lakkaraju, E. Zeitler and A. Bocarsly, *Top. Catal.*, 2014, 1.
22 *Handbook of Electrochemistry*, ed. C. G. Zoski, Elsevier, Amsterdam, 2007.
23 J. F. Endicott and H. Taube, *Inorg. Chem.*, 1965, **4**, 437.
24 T. Gennett and M. J. Weaver, *Anal. Chem.*, 1984, **56**, 1444.
25 R. K. Jaworski and R. L. McCreery, *J. Electroanal. Chem.*, 1994, **369**, 175.
26 H. S. Lim, D. J. Barclay and F. C. Anson, *Inorg. Chem.*, 1972, **11**, 1460.
27 T. J. Meyer and H. Taube, *Inorg. Chem.*, 1968, **7**, 2369.
28 D. O. Wipf, E. W. Kristensen, M. R. Deakin and R. M. Wightman, *Anal. Chem.*, 1988, **60**, 306.
29 K. Yasukouchi, I. Taniguchi, H. Yamaguchi and M. Shiraishi, *J. Electroanal. Chem. Interfacial Electrochem.*, 1979, **105**, 403.
30 M. Jitaru, *J. Univ. Chem. Technol. Metall.*, 2007, **42**, 333.
31 L. A. Dick, A. D. McFarland, C. L. Haynes and R. P. Van Duyne, *J. Phys. Chem. B*, 2001, **106**, 853.
32 D. L. Jeanmaire and R. P. Van Duyne, *J. Electroanal. Chem. Interfacial Electrochem.*, 1977, **84**, 1.
33 S. M. Angel, L. F. Katz, D. D. Archibald, L. T. Lin and D. E. Honigs, *Appl. Spectrosc.*, 1988, **42**, 1327.
34 R. P. Van Duyne, in *Chemical and Biochemical Applications of Lasers*, ed. C. B. Moore, Academic Press, 1979, p. 101.
35 J. A. Creighton, *Surf. Sci.*, 1986, **173**, 665.
36 W.-B. Cai, C.-X. She, B. Ren, J.-L. Yao, Z.-W. Tian and Z.-Q. Tian, *J. Chem. Soc., Faraday Trans.*, 1998, **94**, 3127.
37 A. J. Lucio and S. K. Shaw, *J. Phys. Chem. C*, 2015, **119**, 12523.
38 R. Piontelli, U. Bertocci, G. Poli, G. Serravalle, N. Pentland, J. O. M. Bockris and E. Sheldon, *J. Electrochem. Soc.*, 1958, **105**, 752.
39 D. Marin, F. Medicuti and C. Teijeiro, *J. Chem. Educ.*, 1994, **71**, A277.
40 J. O. M. Bockris, *Chem. Rev.*, 1948, **43**, 525.
41 J. O. M. Bockris, I. A. Ammar and A. K. M. S. Huq, *J. Phys. Chem.*, 1957, **61**, 879.
42 E. Santos, P. Quaino and W. Schmickler, *Phys. Chem. Chem. Phys.*, 2012, **14**, 11224.
43 J. Zhou, Y. Zu and A. J. Bard, *J. Electroanal. Chem.*, 2000, **491**, 22.
44 J. Barber, S. Morin and B. E. Conway, *J. Electroanal. Chem.*, 1998, **446**, 125.
45 N. M. Markovica, S. T. Sarraf, H. A. Gasteiger and P. N. Ross, *J. Chem. Soc., Faraday Trans.*, 1996, **92**, 3719.
46 C. Costentin, J. C. Canales, B. Haddou and J.-M. Savéant, *J. Am. Chem. Soc.*, 2013, **135**, 17671.
47 L. R. F. Allen Bard, *Electrochemical Methods: Fundamentals and Application*, John Wiley & Sons inc, New York, 2nd edn, 2001.
48 E. Skulason, G. S. Karlberg, J. Rossmeisl, T. Bligaard, J. Greeley, H. Jonsson and J. K. Norskov, *Phys. Chem. Chem. Phys.*, 2007, **9**, 3241.
49 B. E. Miller, *Surface Enhanced Raman Scattering of Composition Modulated Alloys and Surface and Solution Raman Scattering in the Visible and Ultraviolet*, Northwestern University, 1989.

 